International Journal of Fluid Machinery and Systems
Vol. 9, No. 2, April-June 2016

DOI: http://dx.doi.org/10.5293/IJFMS.2016.9.2.129
ISSN (Online): 1882-9554

Original Paper

Performance Research of Counter-rotating Tidal Stream Power Unit

Xuesong Wei[1], Bin Huang[2], Pin Liu[2] and Toshiaki Kanemoto [2]

[1] Faculty of Engineering, Kyushu Institute of Technology Kitakyushu 804-0015, Japan,
Research student from Zhejiang University, Hangzhou 310027, China, 11228020@ zju.edu.cn
[2] Faculty of Engineering, Kyushu Institute of Technology Kitakyushu 804-0015, Japan,
huang.bin404@mail.kyutech.jp, liu.pin379@mail.kyutech.jp, kanemoto.toshiaki886@mail.kyutech.jp

Abstract

An experimental investigation was carried out to improve the performance of a counter-rotating type horizontal-axis tidal stream power unit. Front and rear blades were designed separately based on modified blade element momentum (BEM) theory, and their performances at different conditions of blade tip speed ratio were measured in a wind tunnel. Three different groups of blades were designed successively, and the results showed that Group3 possessed the highest power coefficient of 0.44 and was the most satisfactory model. This experiment shows that properly increasing diameter and reducing chord length will benefit the performance of the blade.

Keywords: counter-rotating, tidal turbine, power coefficient, wind tunnel, BEM

1. Introduction

Renewable energy derived from tidal stream has been becoming increasingly popular in the 21st century as an acceptable substitute for conventional resources. Marine currents are primarily driven by the tides (i.e. tidal currents or tidal streams) which occur because of the variation in level of the surface of the sea caused by interaction of the gravitational fields of the Moon and to a lesser extent the Sun with the Earth [1]. Compared with fossil fuels and nuclear power, energy from tidal stream is provided with far less pollution and enhanced security level. In the meantime, the market for green energy is developing in various areas of the world, where tidal stream occupies an important position. A special advantage of tidal stream is that it's predictable, which is beneficial to the reliability and efficiency of tidal turbines. The horizontal-axis tidal turbine, known as HATT, is one of the most important devices extracting energy from the tidal stream.

In most cases so far, marine current turbine prototypes closely follow conventional wind turbine practice, with 2- or 3-bladed horizontal-axis rotors [2]. There exists some similarity between wind turbine and tidal turbine, but the difference of flow characteristics still requires special consideration. In order to improve the performance, the concept of counter-rotating emerged and was applied to tidal turbine. Compared with traditional ones with single rotor, the counter-rotating turbines with two co-axial rotors possess fruitful advantages [3]:

(1) The output and relative rotational speed are sufficiently higher, and may be easy to cope with cavitation because its rotational speed decreases by half while the armature diameter and the induced voltage are the same as those of the traditional tidal turbine.

(2) The rotational moment rarely acts on the pillar because the moments of both propellers/armatures are counter-balanced in the unit.

(3) The flow has no swirling component behind the unit, because the swirling velocity component induced from the front propeller must be absorbed by the rear propeller.

As a result, the counter-rotating type horizontal tidal turbine is blessed with significant value and wide application foreground. Previously, some satisfactory results have been achieved from the investigations of counter-rotating type HATT. Kanemoto T etc. [4, 5] designed the "Counter Rotating Type Hydroelectric Unit" which was composed of the axial flow type tandem runners and the peculiar generator with the double rotational armatures. The unit was operated at the on-cam condition. Usui Y etc. [3, 6] applied experimental researches on the performances of counter-rotating tidal turbines with both mooring and pillar systems and investigated the effects of the propeller rotation on the sea surface. Huang B etc. designed a CFD model for the design of the counter-rotating type HATT which achieved good agreements with the experiment results [7], and developed an optimization method for blade pitch angles of the dual rotors both numerically and experimentally [8].

In this paper, different kinds of counter-rotating tidal turbine blades were designed by modified blade element momentum (BEM)

Received October 20 2015; accepted for publication December 19 2015: Review conducted by Tadashi Tanuma, Ph.D. (Paper number O15056S)
Corresponding author: Bin Huang, huang.bin404@mail.kyutech.jp

This paper was presented at 13th Asian International Conference on Fluid Machinery (AICFM), September 7-10, 2015, Tokyo, Japan

theory in order to get the performance improved. The experiment was conducted in the wind tunnel and the power coefficient was achieved under various blade tip speed ratios.

2. Design methodology of counter-rotating tidal turbine

Blade Element-Momentum (BEM) theory is one of the most commonly accepted methods for calculating induced velocities on wind turbine blades [9, 10, 11]. It is composed of two separate theories, momentum theory and blade element theory. Momentum theory refers to a control volume analysis of the forces at the blade based on the conservation of linear and angular momentum. Blade element theory refers to an analysis of forces at a section of the blade, as a function of blade geometry. Figure 1 shows detailed information about the velocity and force distribution of single blade element.

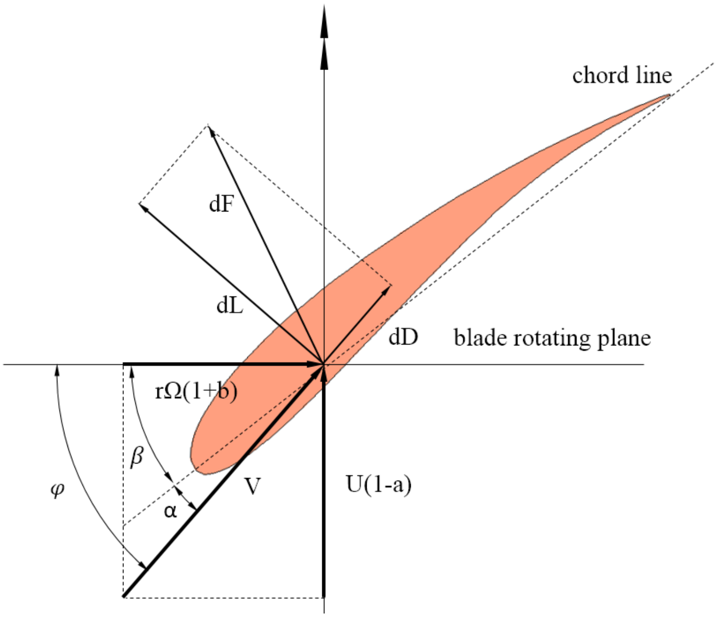

Figure 1 Force and velocity distribution for single blade element

Where, a is axial velocity reduction factor representing the fractional decrease of flow velocity from the free stream to the blade plane, so the flow velocity in the rotor plane is U(1-a), and b is tangential velocity reduction factor representing the influence of the annular torque exerted by the rotor on the flow. The flow behind the rotor rotates oppositely with the angular velocity ω, and the relative tangential velocity of the flow in the rotor plane is $r\Omega(1+b)$, where $b=\omega/2\Omega$.

The axial force and the angular momentum acting on the flow stream which are derived from momentum theory are shown in eq. (1) and eq. (2) respectively.

$$dT = \rho U^2 4a(1-a)\pi r dr \tag{1}$$

$$dQ = 4b(1-a)\rho U \pi r^3 \Omega dr \tag{2}$$

The axial force and the angular momentum acting on the blade element which is derived from momentum theory is shown in eq. (3) and eq. (4) respectively.

$$dT = \sigma\pi\rho \frac{U^2(1-a)^2}{\sin^2\varphi}(C_l \cos\varphi + C_d \sin\varphi) r dr \tag{3}$$

$$dQ = \sigma\pi\rho \frac{U^2(1-a)^2}{\sin^2\varphi}(C_l \sin\varphi - C_d \cos\varphi) r^2 dr \tag{4}$$

The forces and moments derived from momentum theory and blade element theory must be equal, so we can get eq. (5) and eq. (6) as follows:

$$\frac{a}{1-a}\sin^2\varphi = \sigma\frac{C_N}{4} \tag{5}$$

$$\frac{b}{1+b}\cos\varphi\sin\varphi = \sigma\frac{C_T}{4} \tag{6}$$

Where $C_N = C_l \cos\varphi + C_d \sin\varphi$, $C_T = C_l \sin\varphi - C_d \cos\varphi$, C_N is axial force coefficient and C_T is tangential force coefficient. The equations are solved by iterative computation until a and b get converged values considering blade tip losses, then the flow condition can be obtained, which will be integrated over all the blades to predict the performance of the entire rotor.

But for the case of counter-rotating turbines, the flow conditions become more complicated as a result of the existence of the rear blade, as shown in Fig.2. There are more unknown variables than equations, and the blade element momentum theory must be modified. Considering the practical situations, the modifications can be made under certain assumptions:

(1) The distance between the front rotor and the rear rotor is negligible, which means the two rotors can be treated as one actuator disk.

(2) The swirl caused by the front rotor is removed by the rear rotor, leaving tangential inflow factor to be zero at the rear rotor exit.

(3) The axial thrust loadings on the two rotors are supposed to be equal.

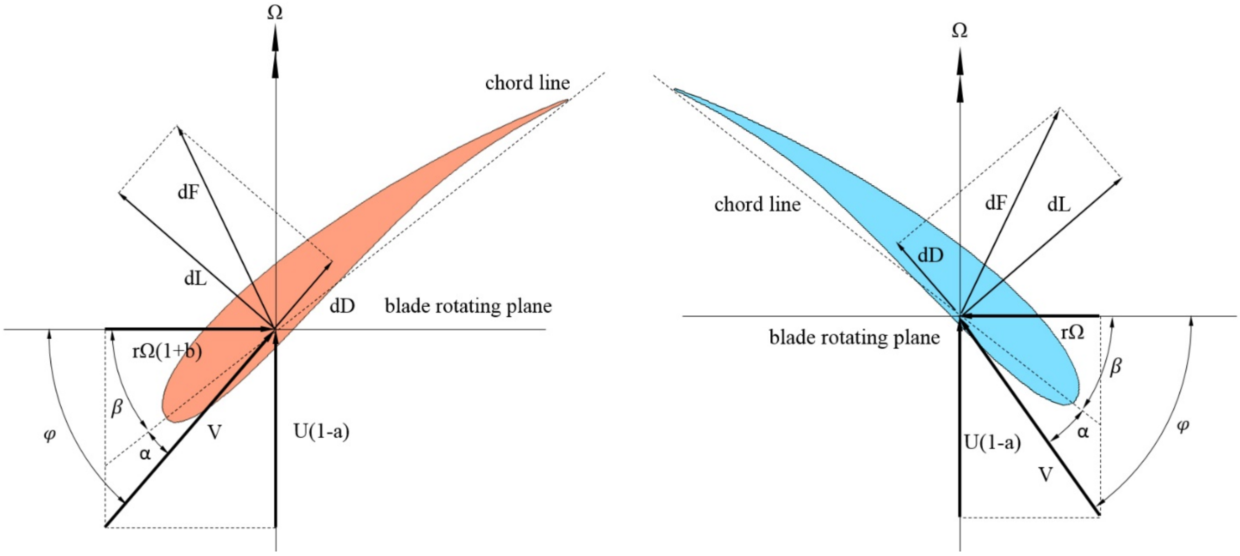

(a) Front blade (b) Rear blade

Figure 2 Detailed information of force and velocity for the counter-rotating blades

For the front rotor, the blade only experiences half of the total axial force caused by the flow, so the axial momentum equation will be changed to:

$$\frac{a}{1-a}\sin^2\varphi = \sigma\frac{C_N}{2} \tag{7}$$

And for the rear rotor, because the swirl is removed, the tangential relative velocity becomes $r\Omega$, and the tangential equation will be changed to:

$$b\cos\varphi\sin\varphi = \sigma\frac{C_T}{4} \tag{8}$$

3. Experimental instrumentation and procedure

One front blade (F) and three different rear blades (R1, R2 and R3) were designed using elements interpolated from three kinds of hydrofoils which were shown in Fig.3. The structure of the blades were shown in Fig.4.

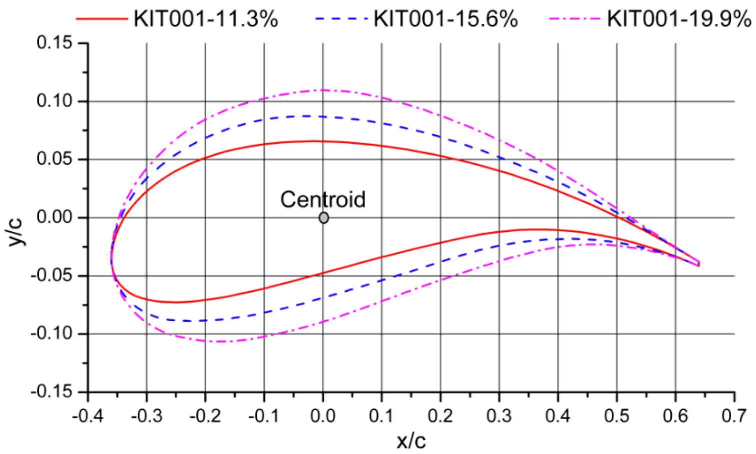

Figure 3 Hydrofoils used in this research

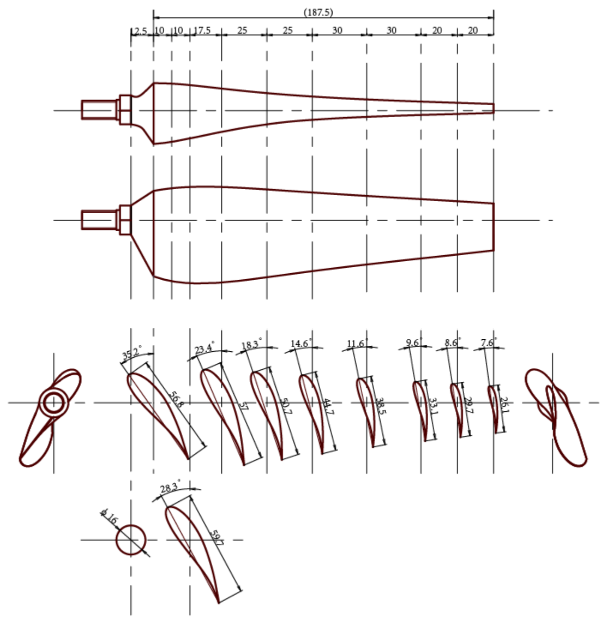

(a) Front blade (F)

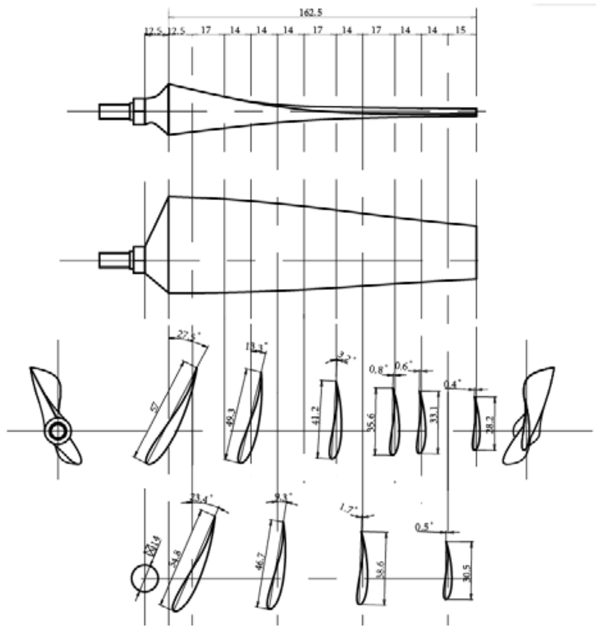

(b) Rear blade (R1)

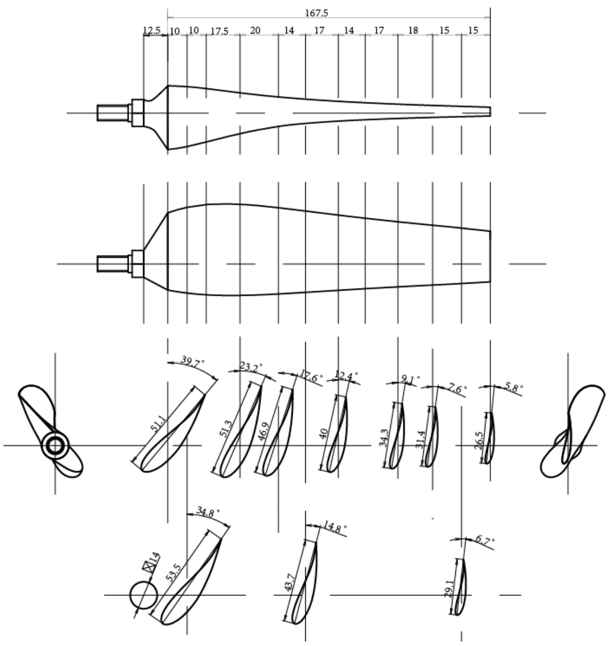

(c) Rear blade (R2)

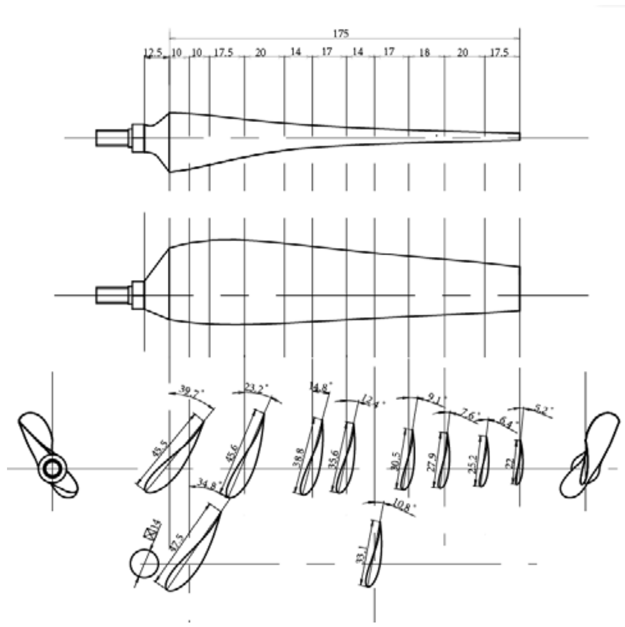

(d) Rear blade (R3)

Figure 4 Blade profiles of the test model

The instrumentation is composed of the test model, the control system and the measurement system. For the test model, the blades are attached to a cone hub with a base diameter of 90 mm and were fixed by bolts so that the blade pitch angle can be adjusted conveniently. The hub is divided into three parts, as shown in Fig.6, to allow the counter-rotating of the two co-axial rotors. The control system includes two motors with regenerative braking system. The front rotor was attached to the inner shaft which was connected to Motor 1 directly, whereas the rear rotor was attached to the outer shaft which was connected to Motor 2 using a belt. Bolts were applied for axial fixation. The inner shaft and the outer shaft are concentric and are provided respectively with a measurement system including a torque detector and a rotation detector.

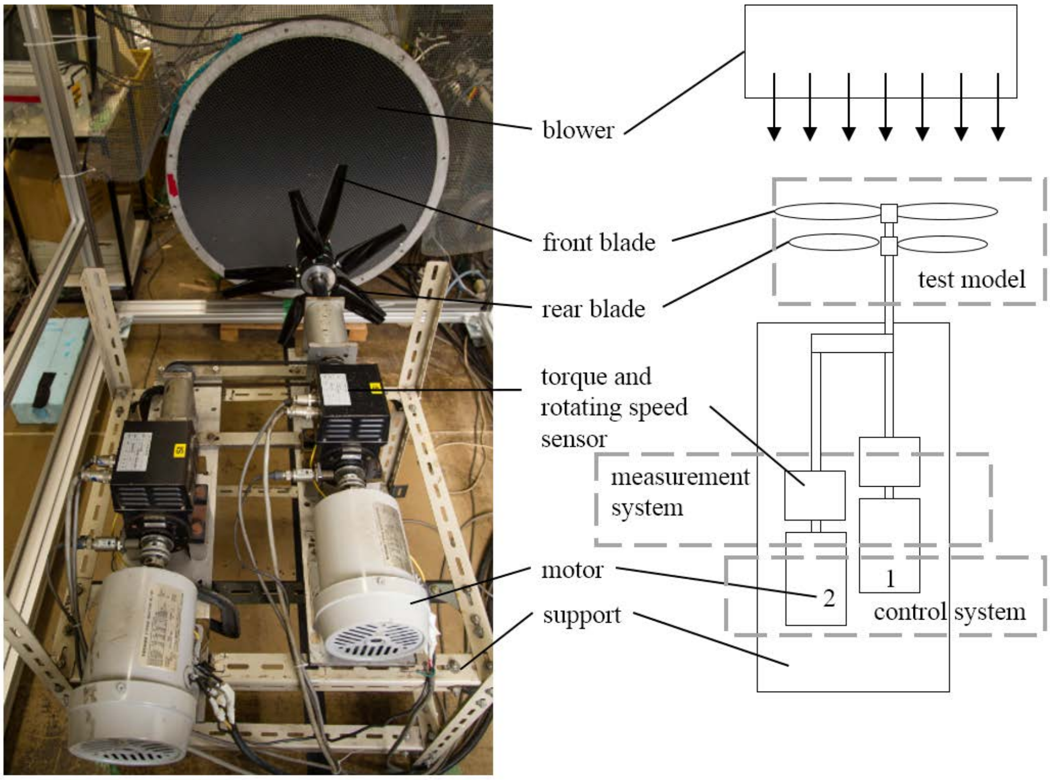

Figure 5 Photograph and of schematic experimental instrumentation

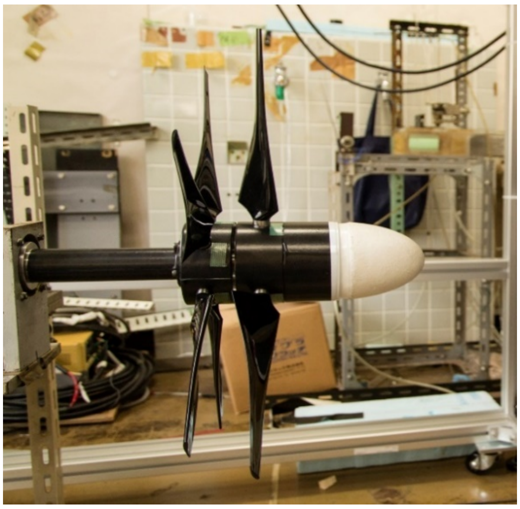
Figure 6 Detailed structures of the hub

The blower worked at the frequency of 36 Hz, and the wind speed was 10m/s which was measured by flow velocity probe. The values of wind speed, rotor's rotating speed as well as rotor's torque would be recorded only when the torque of the upstream rotor and the downstream rotor equaled each other. Finally the power coefficient C_P was calculated as follow:

$$C_P = \frac{P}{\frac{1}{2}\rho A U^3} \tag{9}$$

The torque detector Model SS-050 was produced by Ono Sokki, with torque measurement range of 5 Nm and minimum resolution of 0.001Nm. The accuracy is ±0.2% of full scale. The rotation detector MP-981, which was also produced by Ono Sokki, is able to measure the rotational speed from 0 to 20000 rpm with accuracy of ±0.02% of full scale. The flow velocity probe, testo 435, can detect the wind speed from 0.6 to 40 m/s with accuracy of ± (0.2 m/s +1.5% of measured value). The high-precision equipment is a guarantee of the experiment results.

4. Results and discussion

The experiment was divided into three groups: Group1 (Blade F and Blade R1), Group2 (Blade F and Blade R2) and Group3 (Blade F and Blade R3). The torque was measured under the optimal blade pitch angles to get the best power coefficient. The results are as follows:

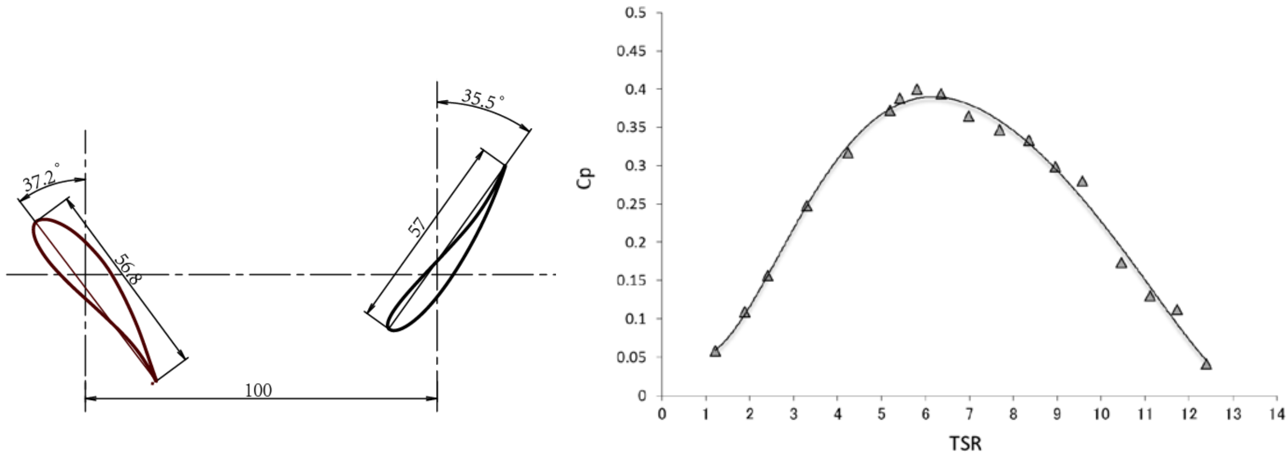

Figure 7 Blade pitch angels and performance of Group1

From Fig.7 it can be found that the power coefficient curve possesses a parabolic shape and the largest value 0.40 occurs when tip speed ratio reaches 5.8, which is not very satisfactory. The TSR ranges from 4.6 to 7.8 where C_p exceeds 0.35, and ranges from 3.3 to 9.7 where C_p exceeds 0.25.

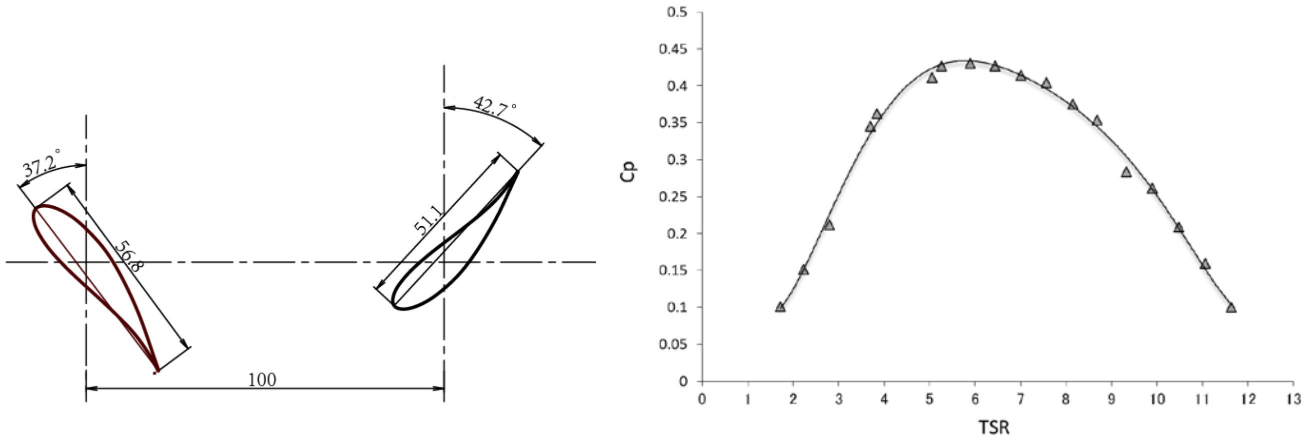

Figure 8 Blade pitch angels and performance of Group2

In Group2 Blade R1 was replaced by Blade R2 whose diameter is 3%longer than that of Blade R1. When TSR reaches 5.9, C_p reaches the maximum value of 0.43 which was 7.5% higher than that of Group1. The TSR ranges from 3.8 to 8.6 where C_p exceeds 0.35 and ranges from 3 to 10 where C_p exceeds 0.25. The high performance range was significantly enhanced.

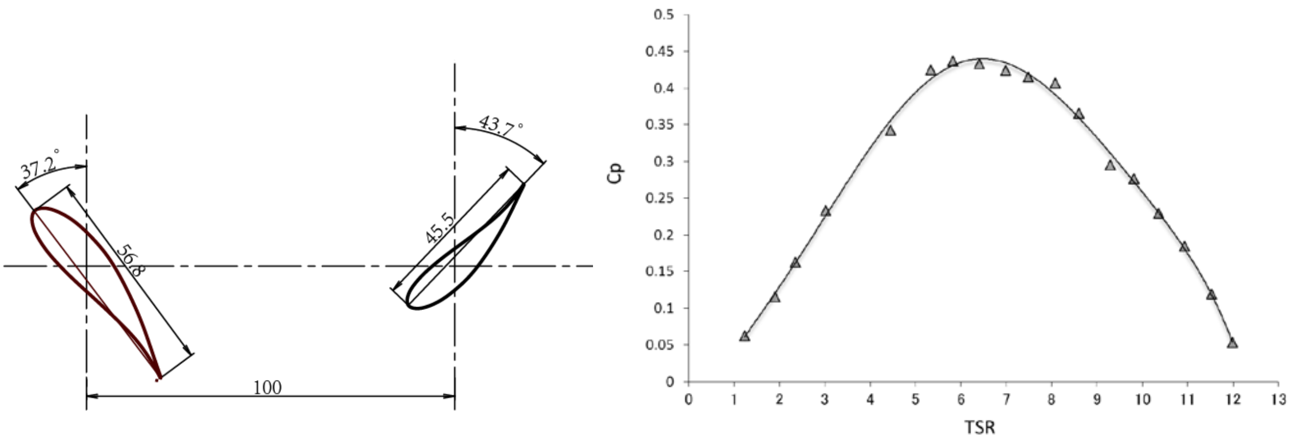

Figure 9 Blade pitch angels and performance of Group3

In Group3 Blade R2 was replaced by Blade R3 whose diameter is 8%longer than that of Blade R1. The maximum value of C_p reaches 0.44, when TSR reaches 5.8. The TSR ranges from 4.3 to 8.7 where C_p exceeds 0.35 and ranges from 3.3 to 10.2 when C_p exceeds 0.25.These areas are slightly smaller than those of Group2, but the area where C_p exceeds 0.4 is from 5.1 to 7.9 while in Group2 this area is from 4.5 to 7.5. So Group3 tends to operate efficiently at higher TSR than Group2.

Figure 10 shows the summary of the performance of three groups. Group3 has the highest C_p value and relatively wide high performance range, which is the most satisfactory model. The rear blade in Group3 has the largest diameter and shortest chord length, which is beneficial to increasing the front face area and reducing weight.

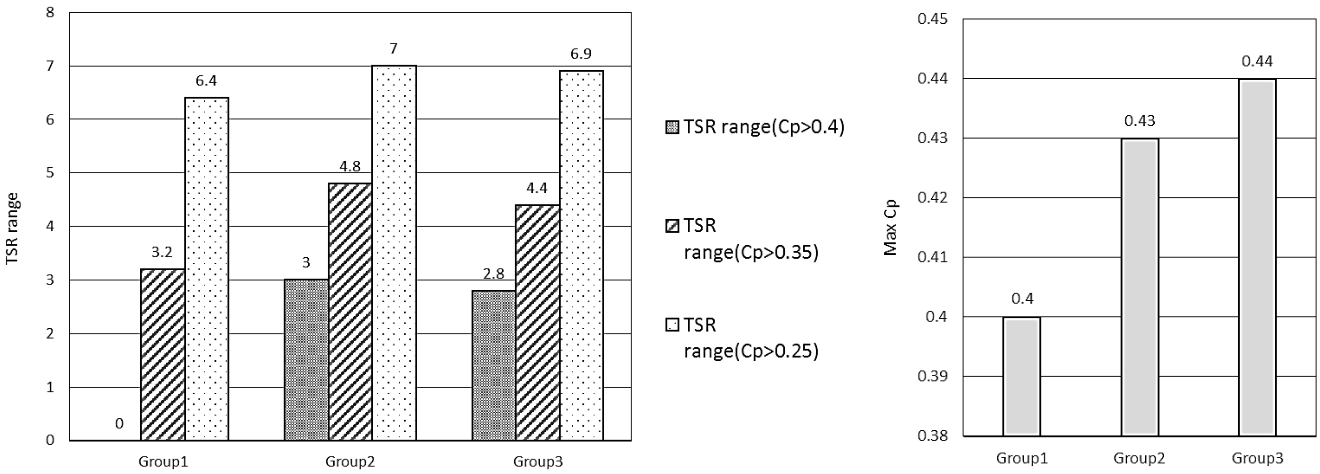

Figure 10 Comparison of results from three groups

5. Conclusion

This paper deals with the performance improvement of counter-rotating type horizontal-axis tidal stream power unit. Three groups of blades were designed based on modified blade element momentum (BEM) theory, and their performances at different conditions of blade tip speed ratio were experimentally investigated. Group3 possesses the highest power coefficient and relatively wide high performance range, which is the most satisfactory result among all three groups. It can be concluded that properly increasing diameter and reducing chord length will benefit the performance of the blade.

Acknowledgments

The authors wish to thank the New Energy and Industrial Technology Development Organization in Japan for their kind and vigorous support.

Nomenclature

A	rotor area	P	power
a	axial velocity reduction factor	r	blade element radius
b	tangential velocity reduction factor	U	mean flow speed
C_d	drag coefficient	V	relative velocity
C_l	lift coefficient	α	angle of attack
C_N	axial force coefficient	β	section pitch angle
C_p	power coefficient	ρ	fluid density
C_T	tangential force coefficient	σ	rotor solidity
dD	drag force	φ	angle of relative flow
dF	total force	Ω	angular velocity of rotor
dL	lift force		

Abbreviation

BEM	blade element momentum	*TSR*	tip speed ratio
HATT	horizontal-axis tidal turbine		

References

[1] Fraenkel, P. L., 2002, “Power from marine currents,” Proceedings of the Institution of Mechanical Engineers, Part A: Journal of Power and Energy, Vol. 216, No. 1, pp. 1-14.

[2] Myers, I. and Bahaj, A. S., 2004, “Basic operational parameters of a horizontal axis marine current turbine,” In Proceedings of World Renewable Energy Congress, Denver, USA.

[3] Usui, Y., Kanemoto, T., & Hiraki, K., 2013, “Counter-rotating type tidal stream power unit boarded on pillar (performances and flow conditions of tandem propellers),” Journal of Thermal Science, Vol. 22, No.6, pp. 580-585.

[4] Kanemoto, T., et al., 2000, "Counter-rotating type machine suitable for tidal current power generation," The Tenth International Offshore and Polar Engineering Conference. International Society of Offshore and Polar Engineers.

[5] Kanemoto, T., and T. Suzuki, 2010, "Counter rotating type hydroelectric unit suitable for tidal power station," IOP Conference Series: Earth and Environmental Science. Vol. 12. No. 1. IOP Publishing.

[6] Usui, Yuta, et al., 2013, "Counter-rotating type tidal-stream power unit playing favorable features in various ocean circumstances," ASME 2013 International Mechanical Engineering Congress and Exposition. American Society of Mechanical Engineers.

[7] Huang Bin, Usui Yuta, Takaki Kohei, et al., 2014, “Numerical and experimental analysis of a counter-rotating type horizontal-axis tidal turbine,” The 6th International Symposium on Fluid Machinery and Fluids Engineering, Wuhan, China.
[8] Huang Bin, Usui Yuta, Takaki Kohei, et al., 2014, “Optimization of blade pitch angles of a counter-rotating type horizontal-axis tidal turbine using response surface methodology and experimental validation,” The 4th Asia-Pacific Forum on Renewable Energy, Yeosu, Korea,.
[9] Manwell J F, McGowan J G, Rogers A L., 2010, Wind energy explained: theory, design and application, John Wiley & Sons, New York.
[10] Moriarty, P. J., & Hansen, A. C., 2005, AeroDyn theory manual, National Renewable Energy Laboratory. Golden, Colorado.
[11] Burton, T., Sharpe, D., Jenkins, N., & Bossanyi, E., 2001, Wind energy handbook, John Wiley & Sons, New York.